A Structural Transformation Integrated Assessment Model of Climate Change

Johannes Koch* Marian Leimbach† Marcos Marcolino

DRAFT: NOT FOR PUBLICATION

Abstract

We develop a global scale structural transformation integrated assessment model to study the interaction between the sectoral reallocation of economic activity with climate change and mitigation policies. We find that in most regions, global coordination in face of climate damages shifts economic activity out of the manufacturing and into the services sector, which is less energy intensive and can more easily substitute between energy sources. The exception is Sub-Saharan Africa, where we observe an increase in manufacturing in the early period to increase investment. Compared to an uncoordinated world, coordination comes with a decrease in global emissions, welfare gains for developing regions, and a decrease in emission intensity in all regions: peak global emissions are reduced by 25%, welfare increases by 3.4% and 4.0% in India and Sub-Saharan Africa respectively, and the emission intensity decreases by 8% in Sub-Saharan Africa and 27% in the United States. The role of structural change in the reduction of emission intensity is varied, accounting between 1.5% and 37% of the decline depending on the region, yet always secondary to the role of sector-level efficiency improvements. Structural change analyses of impact and mitigation scenarios show that changes to the sectoral composition are small, yet asymmetric across low- and high-income regions. An increase in damages leads to an increase of the agricultural sector in low-income regions, but not in high-income regions, while the decarbonization of the energy sector leads to an increase of the agricultural sector in high-income regions but not in low-income regions.

Keywords: structural transformation; multi-sector model; integrated assessment; climate change

*Potsdam Institute for Climate Impact Research. E-mail: jokoch@pik-potsdam.de.
†Potsdam Institute for Climate Impact Research. E-mail: leimbach@pik-potsdam.de.

1 Introduction

Structural transformation refers to the reallocation of economic activity across broad sectors of the economy, a well-known characteristic that accompanies the process of economic growth[1]. It is commonly defined as the reallocation of output and workers across the agriculture, manufacturing and services sectors: as income grows, the shares of output and workers decline in agriculture, increase in services, and follow a hump shape (increasing at lower levels of income and decreasing at higher) in manufacturing.

The transformation from an agrarian-based economy to an industrialized and service-oriented one is often associated with improvements in productivity, technological advancements, and rising living standards. Economic growth has also been associated with an increase in energy use and greenhouse gas emissions, specifically CO2 [2]. After all, energy is an indispensable input of production and its use the main source of anthropogenic CO2 emissions[3], emissions that are responsible for increasing the global average temperature and changing the climate in a significant and hazardous manner.

How climate change will impact our economies, and how it might be mitigated, have become two of the most pressing questions of our time. And yet, while the interactions between climate change and the economy as a whole have been studied extensively (see IPCC (2024)), research on the interactions between climate change and structural change remains scarce. In an extensive review of the modelling landscape, Ciarli and Savona (2019) find that most economic modelling approaches, including integrated assessment models (IAMs), cover at best only certain aspects of the interaction between structural change and climate change[4].

Integrated Assessment Models (IAMs) are a widely used tool to analyze the interactions between the economy and climate system. They differ in their complexity and can range from medium-size models such as the DICE and RICE models (Nordhaus (1992b); Nordhaus and Yang (1996)) to large scale process-based models (e.g.AIM, GCAM, IMAGE, MESSAGE, REMIND - Riahi et al. (2017)). In general, however, IAMs do not endogenize the sectoral reallocation of economic activity, and hence do not address the role of structural change[5]. Yet, different economic sectors are expected to be heteroge-

[1]The process of structural transformation has been thoroughly discussed in the economic literature, see Maddison (1980) and Herrendorf et al. (2014)

[2]For a comprehensive review of the literature, see Fávero et al. (2022).

[3]The other main sources of CO2 emissions are direct industrial processes (e.g. cement and chemical production) and land use, land use change and forestry (LULUCF) IPCC (2024).

[4]Ciarli and Savona (2019) identify six aspects of structural change that affect climate change: sectoral composition, industrial organisation, technology, employment, final demand, and institutions. They compare integrated assessment models (IAM), computable general equilibrium (CGE) models, structural change models (SCM), ecological macroeconomics models in the Keynesian tradition (EMK) and evolutionary agent based models (EABM), regarding the degree to which these aspects of structural change are implemented.

[5]A noteworthy exception is the work by Lefèvre et al. (2022), who apply multi-sectoral IAMs to assess the sectoral composition of global and regional economies in the 2°C scenario. The authors find

neous both in their reaction to climate change damages and in their mitigation potential, i.e. the scale and ease at which their greenhouse gas emissions can be reduced. Thus, economic composition is crucial in understanding the impacts of climate change and mitigation policies.

In this paper, we develop a global scale structural transformation integrated assessment model to study the interaction between the sectoral reallocation of economic activity with climate change and mitigation. We analyze the role of sectoral reallocation in reducing emission and how the sectoral composition is affected by increasing damages and a decarbonized energy system.

Sectoral resolution is important to assess the impacts of climate change, because the economic sectors are expected be affected differently. Disproportionate temperature increases can have significant impacts in agriculture and manufacturing, which are the predominant sectors in low-income countries still at early stages of development. As such, low-income will suffer the adverse effects of climate change more intensely than high-income countries. This becomes particularly severe in face of the "food problem": until countries can produce a sufficient amount of food, labor is trapped in agriculture and cannot start the process of modern economic growth[6], a situation likely reinforced in face of climate change. Additionally, the manufacturing sector is also expected to face substantial repercussions from rising temperatures. Some of its production tasks are composed of outside activities, such as construction and mining, which are susceptible to climate conditions.

Sectoral resolution also matters with regard to climate change mitigation, because different sectors have different mitigation potentials. Sectors have different energy intensities and can switch energy source more or less easily. The services sector for example, is often the least energy-intensive sector, with energy expenditure representing only a small share of a firm's cost, and simultaneously the sector that can most readily substitute energy sources between each other. On the other hand, manufacturing is more energy-intensive, and the different energy sources (like heat, liquid fuels, solids, gases and electricity) are linked to specific technological processes and only rarely easily interchangeable[7].

The structural change process is commonly explained by two drivers: changes in consumption preferences with increasing income, i.e. non-homothetic preferences, and unequal productivity growth across the sectors. García-Santana et al. (2021) also considers the change in the investment rate as an an additional driver. The authors document that consumption and investment goods have different sectoral composition, with investment

that climate policies have small impacts in the economic structure, but significant effects inside specific sectors.

[6]The food problem idea dates back to Schultz (1953).

[7]Madeddu et al. (2020) present a comprehensive report on the electrification potential of the European industry sector. They find that close to 80% of the sector's energy demand is, technically, electrifiable with technologies that exist today. However the extent to which this is economically feasible is less certain and depends strongly on the relative prices of the electrification technologies.

being more manufacturing-intensive compared to consumption. This finding suggests that changes in the investment rate can influence the pace and direction of structural change. When the investment rate increases, it implies a greater allocation of resources towards investment goods, which tend to have a higher proportion of manufacturing activities. As a result, the manufacturing sector may experience an expansion.

In our model, structural change is endogenous and driven by both demand and supply side characteristics. On the demand side, the model features non-homothetic preferences. On the supply side the model features different productivities and damage parameters across sectors. Moreover, following García-Santana et al. (2021), investment in our model is more reliant on production in the manufacturing sector than consumption is.

The model and approach in this study differs from Lefevre at al. (2021) in two respects. First, we apply a different type of multi-sectoral model - in contrast to the recursive dynamic models in Lefevre at al., ours is an intertemporal optimization model. Second, whereas Lefevre at al. analyzed effects from climate policy only, we address effects from climate change policy and climate change impacts.

Our analysis relies on the comparison between four distinct scenarios. In the first analysis, analysis we compare a scenario without global coordination and a scenario with global coordination. The results suggest that a globally optimal allocation provide gains for developing regions, such as Sub-Saharan Africa, with the developed regions bearing most of the burden of emissions reduction. Regional emission intensity is reduced through sectoral reallocation and reduction of sectoral emission intensity, the latter of which is the more dominant channel. Most the of the emissions intensity reduction on the sector level happens in the services sector, since it is easier to adopt clean energy inputs in the services sector than in the manufacturing sector. In a second analysis we look at the effect of increased damages from climate change. The results suggest that the response to an increase in damages is asymmetric (mainly regressive) across region groups classified by their stage of development. Finally we analyse the effect of a decarbonized energy system on sectoral allocations. The results suggest, that the response in the agricultural sector is once again asymmetric (slightly progressive).

The remaining of the paper is structured in the following way. In Section 2 we introduce the model, its equations and solution concepts. In Section 3 we describe the calibration of the model parameters. In Section 4, we present our model results and scenario comparison. Finally, Section 5 concludes.

2 Description of the model

The model integrates economic activity with carbon emissions and climate change. The world is divided in twelve regions[8], and each region has three production sectors: agriculture (a), manufacturing (m), and services (s). The production function of each region requires capital k_{it}, labor l_{it} and energy e_{it}. The model is expressed in per employee terms, with emissions being the only exception. Each region is endowed with an initial capital stock, and both capital and labor are freely mobile across sectors. Each region has a representative household that consumes agricultural, manufacturing and services goods, with non-homothetic preferences. There is no trade between regions.

CO2 emissions are a byproduct of energy use that contribute to the elevation of the global mean temperature. The elevation in the temperature creates a climate externality in the form of output loss and its magnitude is sector- and region-specific.

2.1 Household

In each region j, the representative household has preferences represented by the logarithmic utility:

$$U_j = \sum_{t=0}^{\infty} \beta^t \ln(c_{jt}) \tag{1}$$

where $\beta < 1$ is the inter-temporal discount factor and t the time index. The aggregate consumption index c_{jt} combines sectoral goods, c_{it} for $i \in \{a, m, s\}$, into the region's overall consumption[9] according to the non-homothetic Stone-Geary aggregator:

$$c_t = \left[\sum_{i \in \{a,m,s\}} \Omega_i^{\frac{1}{\sigma}} \left(c_{it} + \bar{c}_i\right)^{\frac{\sigma-1}{\sigma}} \right]^{\frac{\sigma}{\sigma-1}} \tag{2}$$

where Ω_i is the weight parameter of good i, $\bar{c}_i$ may represent either a subsistence requirement $\bar{c}_i < 0$ or an endowment $\bar{c}_i > 0$, and σ is an elasticity parameter [10].

2.2 Production

The output of sector $i \in \{a, m, s\}$, y_{it}, is produced using labor l_{it}, capital k_{it} and an energy composite e_{it}. The capital-labor productivity in each sector is denoted by A_{it} and

[8] The regions are: United States (USA), Europe (EUR), China (CHA), Russia and Reforming Economies (REF), India (IND), Japan (JPN), Other Asia (OAS), Middle Eastern and North Africa (MEA), Latin America (LAM), Canada, Australia and New Zealand (CAZ), Sub-Saharan Africa (SSA) and Non-EU European countries (NEU). See Appendix (A.6) for the further description of the mapping between countries and regions.

[9] We exclude the region index j from the math notation whenever there is no ambiguity in the understanding.

[10] Parameter σ is not equal to the elasticity of substitution in the Stone-Geary utility function, due to the presence of $\bar{c}_i$. For further discussion of this point, see Comin et al. (2021).

the energy productivity is represented by A^e_{it}. The production function incorporates the damage impacts of an increase in the global mean temperature and is represented by a function with constant elasticity of substitution (CES) as:

$$y_{it} = D_{it}\left[\theta_i(A_{it}k^{\alpha}_{it}l^{1-\alpha}_{it})^{\frac{\nu_i-1}{\nu_i}} + (1-\theta_i)(A^e_{it}e_{it})^{\frac{\nu_i-1}{\nu_i}}\right]^{\frac{\nu_i}{\nu_i-1}} \tag{3}$$

where D_{it} is a sector-specific damage multiplier on output, $\theta_i \in (0,1)$ with $\sum_{i\in\{a,m,s\}}\theta_i = 1$ the share parameter, and $\nu_i \in [0,\infty)$ the sector-specific elasticity of substitution. The energy composite is a CES function which bundles together electric e^{el}_{it} and non-electric e^{noel}_{it} energy as:

$$e_{it} = \left[\theta^{e\,\frac{1}{\nu^e_i}}_i \left(B^{noel}_{it}e^{noel}_{it}\right)^{\frac{\nu^e_i-1}{\nu^e_i}} + (1-\theta^e_i)^{\frac{1}{\nu^e_i}}\left(B^{el}_{it}e^{el}_{it}\right)^{\frac{\nu^e_i-1}{\nu^e_i}}\right]^{\frac{\nu^e_i}{\nu^e_i-1}} \tag{4}$$

where B^{el}_{it} and B^{noel}_{it} are the type-specific energy productivities, $\theta^e_i \in (0,1)$ with $\sum_{i\in\{a,m,s\}}\theta^e_i = 1$ is the share parameter, and $\nu^e_i \in [0,\infty)$ the sector-specific elasticity of substitution between energy types.

The investment good x_t is produced by combining the sectoral goods x_{it} using a CES production function:

$$x_t = A^x_t\left[\sum_{i\in\{a,m,s\}}(\theta^x_i)^{\frac{1}{\nu^x}}\,x_{it}^{\frac{\nu^x-1}{\nu^x}}\right]^{\frac{\nu^x}{\nu^x-1}} \tag{5}$$

where A^x_t is the exogenous investment-specific technological change, $\theta^x_i \in (0,1)$ with $\sum_{i\in\{a,m,s\}}\theta^x_i = 1$ is the share parameter, and $\nu^x \in [0,\infty)$ is the elasticity of substitution.

The stock of capital in the economy accumulates following the standard law of motion:

$$k_{t+1} = (1-\delta)k_t + x_t \tag{6}$$

where $\delta \in (0,1)$ is the depreciation rate.

2.3 Resource constraints

The sectoral output can be allocated either for consumption or investment, or exchanged for energy at rates ψ^{el}_{it} and ψ^{noel}_{it} [11]. The resource constraint of sector $i \in \{a,m,s\}$ is

$$c_{it} + x_{it} = y_{it} - (\psi^{el}_{it}e^{el}_{it} + \psi^{noel}_{it}e^{noel}_{it}) \tag{7}$$

[11] ψ^{el}_{it} and ψ^{noel}_{it} represent the opportunity cost of each energy source in terms of good i. That is, the amount of good i necessary to get one more unit of energy. Notice that the model does not consider energy supply since the argument is entirely based on final energy demand. See Appendix (A.3) for further discussion on how ψ^{el}_{it} and ψ^{noel}_{it} are pinned down.

Capital and labor are freely mobile across sectors and their resource constraints satisfy:

$$\begin{aligned} k_t &= \sum_{i\in\{a,m,s\}} k_{it} \\ 1 &= \sum_{i\in\{a,m,s\}} l_{it}, \forall t \end{aligned} \tag{8}$$

2.4 Emissions, temperature and damages

Global CO2 emissions emi_t are a byproduct of energy use and are computed using CO2-intensities of the different energy types[12] ξ_t^{el} and ξ_t^{noel}:

$$emi_t = \sum_j \left[L_{jt} \left(\sum_{i\in\{a,m,s\}} \xi_{jt}^{el} e_{jit}^{el} + \xi_{jt}^{noel} e_{jit}^{noel} \right) + emi_{jt}^{other} \right] \tag{9}$$

L_j is the total number of employees per region and is required since e_{it}^{el} and e_{it}^{noel} are expressed per employee. emi_{jt}^{other} is the CO2 emissions from industrial processes (i.e. direct emissions not stemming from energy use in industrial processes) and land-use change[13].

We use the transient climate response to cumulative CO2 emissions (TCRE)[14] ζ, to directly link cumulative global emissions, $emi_t^{cum} = emi_{t-1}^{cum} + emi_{t-1}$ with an increase in global mean temperature W, whereby we abstract away from any delay-effect and assume warming to be an instantaneous function of cumulative emissions:

$$W_t = 1.1\zeta emi_t^{cum} \tag{10}$$

Following Dietz and Venmans (2019) and Allen (2016), we further assume that the total warming induced from CO2 and non-CO2 greenhouse gases together is 10% higher than the warming from CO2 alone, and we multiply ζ by the 1.1 factor.

The damage function is a quadratic function relating temperature increase with percentage output loss:

$$D_{jit} = 1 - (a_{ji}W_t + b_{ji}W_t^2)/100 \tag{11}$$

where a_{ji} and b_{ji} are parameters of the damage function (van der Wijs et al. (2022)).

[12] The CO2-intensities are exogenous and computed using information from the REMIND model. See Appendix (A.4) for further discussion.

[13] The CO2 emissions from industrial processes and land-use change are exogenous and taken from the REMIND model. They represent, in most regions, only a very small share of the total CO2 emissions. See Appendix A.4 for further discussion.

[14] The use of the TCRE is in line with the latest climate science and well established in the literature, see Matthews et al. (2009); Collins et al. (2013); Dietz and Venmans (2019), or MacDougall (2016) for a review. Compared to the climate models with carbon stocks like the ones used by Nordhaus (1992a) or Golosov (2014), the linear climate model based on the TCRE is at the same time much simpler and more accurate.

2.5 Solution concepts

We consider two solution concepts: uncoordinated and coordinated. In the uncoordinated solution, the regions do not internalize the negative effects of their emissions. Each region solves its own problem separately, maximizing its own utility and without internalizing the impacts of its emissions.

In the coordinated solution, the negative effects of emissions are internalized and the regional emissions are globally efficient. Therefore, the emissions are treated cooperatively through the efficient actions of all regions. A global planner chooses the allocation of each region and maximizes the utilitarian welfare function:

$$\mathcal{W} = \sum_t \sum_j \beta^t \omega_{jt} ln(c_{jt}) \tag{12}$$

with utilitarian weights ω_{jt} equal to the population share of region j relative to global population.

3 Calibration

The calibration of the model is performed using parameters from the literature, the model itself, and results from the REMIND model. The REMIND model (Baumstark et al. (2021)) is a global integrated assessment model with a detailed energy system that derives welfare-optimal regional transformation pathways of the energy-economic system subject to climate and sustainability constraints for the time horizon from 2005 to 2100. It is itself calibrated to a chosen Shared Social-Economic Pathway (SSP) scenario. These scenarios comprise different narratives and quantifications of possible futures, including economic and demographic trajectories, and provide a basis for exploring climate-change related challenges in different socio-economic environments (Riahi et al. (2017), Dellink et al. (2017), Koch and Leimbach (2023)). In addition REMIND results depend upon mitigation assumptions that vary between none (a baseline scenario) and stringent emission budgets equivalent with specific temperature targets. To calibrate our benchmark model we use a baseline SSP2 scenario.

From the REMIND model we get scenario, region and time-specific energy and emission information with which we define the energy share parameters (θ^e_{ji}, equal to the average of the corresponding energy type's shares in the model's start and end years), the opportunity costs (ψ^{el}_{jit} and ψ^{noel}_{jit}) and CO2 intensities (ξ^{el}_{jt} and ξ^{noel}_{jt}) of energy. Details of the applied method, that is based on the construction of supply curves, are described in Appendices A.3 and A.4.

3.1 Region and time-independent parameters

The region and time-independent model parameters taken from the literature are summarized in Table 1. These include the values for the elasticity and share parameters in the consumption and investment aggregators (σ, ν_i, Ω_i, θ_i^x), the subsistence consumption levels of the sector goods ($\bar{c}_i$), the elasticity and share parameters of the production function (ν_i, θ_i, α), the elasticity between final energy types (ν_i^e), the discount factor (β), the capital depreciation rate (δ) and the TCRE (ζ).

symbol	description	value
β	discount factor	0.985
δ	capital depreciation rate	0.05
$\bar{c}_i$ [1]	subsistence consumption	a = -0.138, m = 0, s = 0
Ω_i [5]	consumption share parameter	a = 0.002, m = 0.15, s = 0.848
σ [2]	consumption elasticity	0.25
α	capital share	0.3
ν_i [3]	production elasticity	a = 0.28, m = 0.23, s = 0.20
θ_i [3]	production share parameter	a = 0.975, m = 0.925, s = 0.975
ν_i^e [4]	energy elasticity	a = 1.21, m = 0.52, s = 1.21
ν^x [5]	investment elasticity	0.51
θ_i^x [5]	investment share parameter	a = 0.031, m = 0.537, s = 0.432
ζ	TCRE	0.0017616

[1] See Herrendorf et al. (2014).
[2] See Comin et al. (2021). Lowest reported value different from zero.
[3] See Baccianti (2013).
[4] See Stern (2012). In manufacturing the value is based on the unweighted mean of the elasticities between different fossils (coal, oil and natural gas) and electricity. For agriculture and services, the elasticities are based on the unweighted meta results.
[5] See García-Santana et al. (2021).

Table 1: Region and time-independent model parameters

Concerning the consumption elasticity parameter σ, previous works in the structural transformation literature which use the Stone-Geary preferences (such as Herrendorf et al. (2013) and Moro et al. (2017)), report values which are not significantly different from zero for the United States. On the other hand, Comin et al. (2021) use an implicit non-homothetic CES and report values between 0.25 and 0.35 for OECD countries, and between 0.50 and 0.57 when considering both high- and low-income countries. We chose to set σ equal to 0.25, which is the lowest values reported by Comin et al. (2021) still different from zero.

The consumption and investment share parameters are from García-Santana et al. (2021). The aggregate consumption good is much more dependent on the production in the service sector ($\Omega_s = 0.848$) than on production in the manufacturing sector ($\Omega_m =$

0.15), while the aggregate investment good is more dependent on the production in the manufacturing sector ($\theta_m = 0.537$) than on production in the service sector ($\theta_s = 0.432$).

3.2 Damage function

The damage multiplier on output (D_{jit}) relates warming with a percentage output loss. It is computed using a damage function (equation 11) as discussed in van der Wijs et al. (2022) and constructed, with additional sectoral disaggregation, by the ICES model Parrado and de Cian (2014)[15]. The output losses induced by a 3°C warming are shown in Table (2). The damage function inflicts substantial losses across all regions and sectors, apart from small gains in the agricultural sectors in Japan and Non-EU-Europe, and in China's manufacturing sector. Losses are relatively small in high-income regions, while substantial in low-income regions: India (IND), Sub-Saharan Africa (SSA) and Other Asia (OAS) face losses above 10% in all sectors. Furthermore, the vulnerability of sectors to climate change differs between low- and high-income regions. In high-income regions, the services sector tends to be the most affected, while in the low-income regions the manufacturing sector is more severely impacted.

	USA	EUR	CAZ	JPN	NEU	CHA	REF	LAM	MEA	OAS	IND	SSA
Agr	2.80	8.56	5.90	-1,27	-6.61	1.72	0.97	8.31	13.5	16.7	25.2	13.0
Man	5.89	2.62	6.61	7.63	2.67	-5.72	6.70	9.47	5.92	18.4	30.9	38.5
Ser	6.31	6.65	7.67	8.06	5.06	2.32	8.31	7.99	12.3	16.1	19.8	29.3

Table 2: Percentage output loss at 3°C warming

3.3 Exogenous Productivity

We follow the insights of Duarte and Restuccia (2010) and use the model to measure the initial capital-labor (A_{ji}), energy (A^e_{ji}, B^{el}_{ji}, B^{noel}_{ji}) and investment (A^x_j) productivities. This methodology is needed because of the lack of comparable PPP-adjusted value-added data at the sectoral level and limited availability of sectoral capital stock data for a large number of countries[16]. In Appendix (A.2) we further discuss the method.

[15]See website www.icesmodel.org for further description.

[16]The methodology follows Duarte and Restuccia (2010), who calibrate a model for a benchmark economy (United States) to construct comparable cross-country measures of labor productivity per sector, into account. An approach in which the national currency value-added shares are applied to the PPP-adjusted measure of aggregate value-added from the Penn World Tables would be problematic. This approach assumes that the PPP-conversion factor for aggregate output applies to all sectors. In contrast, there is strong evidence that the PPP-conversion factors differ across sectors. In the literature, Bah and Brada (2009), Stefanski (2014), Üngör (2017), Świecki (2017), and Buiatti et al. (2017) also apply the insights from Duarte and Restuccia (2010) to study the process of structural transformation and productivity differences across countries. A key aspect that sets this paper apart is using the Duarte and Restuccia method to compute comparable measures of sectoral energy productivity across countries.

In the first step, we assume the benchmark economy has one energy type (see Appendix A.1.1), and therefore without Equation 4 and without B_i^{el} and B_i^{noel}. With this model, we determine the start-year levels of the remaining 7 productivities A_a, A_m, A_s, A_a^e, A_m^e, A_s^e, and A^x. We solve the model iteratively and adjust the initial productivity levels until the model allocation matches the following 7 targets in the start-year: (1) the labor share in agriculture, (2) the labor share in manufacturing, (3) the GDP, (4) the energy level in agriculture, (5) the energy level in manufacturing, (6) the energy level in services, and (7) the share of investment over GDP[17]. For example, consider the case of the United States and 2015 as start year. The share of labor in agriculture in 2015 is 1.4%. Suppose that, for given initial levels of productivity, the model allocation l_a is 1%. This indicates that model productivity is too high as it requires too little workers to produce agricultural goods. Therefore, we decrease the value of A_a. Analogously, if the model's solution for l_a is higher than 1.7%, then we increase A_a. We continue this process until l_a converges to 1.4%. We follow this idea for all productivity levels until the convergence to the associated target is reached.

In the second step, we determine the productivity growth rates. We assume constant growth rates and we adjust them until the model allocation matches a set of targets in the end-year consistent with the SSP2 scenario.

In the final step, we calibrate the energy-type productivities B_i^{el} and B_i^{noel}. We take A_{it}^e as given from the first and second steps, i.e. we fix them to their values from the solution of the single energy type model, and adjust the B_{it}^{el} and B_{it}^{noel} (see A.2.3). To pinpoint B_{it}^{el} and B_{it}^{noel}, we assume that the value of the energy composite e_{it} in both the single energy type and benchmark models is the same.

4 Results

In this section we ask the following questions: What differences in the allocation of economic activity across sectors exist between a world where the climate externality is not taken into account, and a world where the damages from climate change are internalized and the regional emissions globally efficient? What role does sectoral reallocation play in reducing CO2 emissions? How are sector allocations affected by an increase in climate change damages? And finally, how do sector allocations change following a decarbonization of the energy system? To answer these questions we use our model and compare four simulations or scenarios:

- a benchmark "uncoordinated" scenario
- a benchmark "coordinated" scenario

[17]See Appendix A.2.1 for information on the target data sources.

- an "impact" scenario: a coordinated scenario with increased damages
- a "mitigation" scenario: a coordinated scenario with a decarbonized energy system

All scenarios are from 2015 to 2100 and are calibrated to the baseline SSP2 scenario. In the mitigation scenario, the decarbonized energy system is represented by the exogenous opportunity costs and CO2 intensities associated with a REMIND 2°C warming scenario, which implies lower carbon intensities but higher energy cost terms ψ_{it}^{el} and ψ_{it}^{noel}.

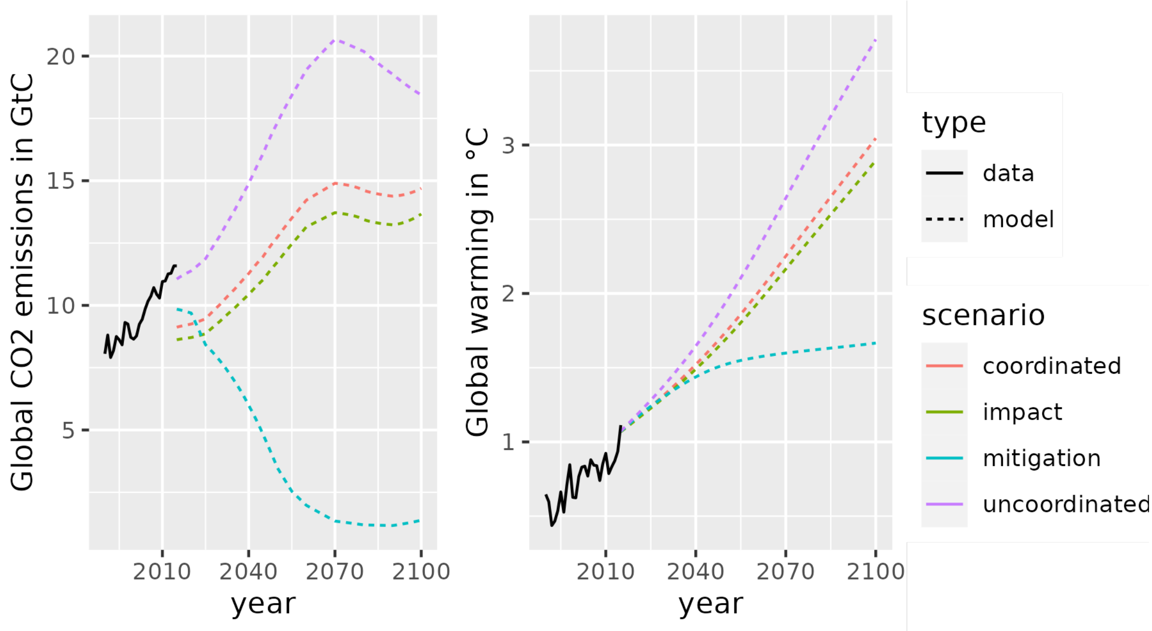

Figure 1: Global CO2 emissions and warming

Note: Figure 1 displays the global CO2 emissions (in gigatons of carbon, GtC) and warming since the pre-industrial era (1880-1900) in °C for the four scenarios: uncoordinated, coordinated, impact and mitigation (dotted colored lines). Historical data on CO2 emissions and warming (from the European Enviornment Agency, see here) from are shown in solid black lines.

Figure 1 shows the global CO2 emissions and temperature increase for the four scenarios. In the uncoordinated scenario, CO2 emissions reach 20 GtC per year in 2070, decreasing slowly thereafter, leading to 3.7°C warming by 2100. The other three scenarios, all of which use the coordination solution concept, have lower emissions and lower temperature increases with the impact scenario having slightly less emissions than the coordinated scenario, and the mitigation scenario having significantly less emissions than both the coordination and impact scenarios. The temperature increases by 2100 for these scenarios are 3.0°C, 2.9°C and 1.7°C for the coordination, impact and mitigation scenarios respectively.

4.1 Global coordination

4.1.1 Welfare

When internalizing the climate externality, the global planner coordinates economic activities such that mitigation efforts are done where they are most efficient and resulting welfare losses are lowest. With respect to the latter, the planner takes into account that in regions with relatively lower income levels the marginal utility of consumption is higher. The welfare impacts of coordination are calculated using the concept of consumption equivalent, which is the fixed percentage of consumption c^{eq} that would make the household of a region indifferent between the uncoordinated solution and the coordinated. It is calculated as:

$$\sum_{t=t_0}^{\infty} \beta^{t-t_0} U\left(c_t^{CO}\right) = \sum_{t=t_0}^{\infty} \beta^{t-t_0} U\left((1+c^{\text{eq}})c_t^{UN}\right) \tag{13}$$

where c_t^{CO} is the aggregate consumption in the coordinated scenario, and c_t^{UN} is the aggregate consumption in the uncoordinated scenario. The coordination scenario yields a global welfare $\mathcal{W}$ gain of 2.2%. However, it is important to note that this gain is not evenly distributed among regions. Table 3 reports the consumption equivalence for each region. We observe that low-income regions benefit the most from coordination. This is intuitive since these regions are expected to bear the highest damages from increasing temperature (see Table 2). India, SSA, MEA, and OAS experience welfare gains ranging from 2% to 4%. On the other hand, high-income regions and China face significant welfare losses. While these regions also benefit from lower damages, efforts of reducing emissions yield losses that overcompensate the benefits. The USA bear the highest welfare losses with a value close to 3%. In particular, notice that the losses for the USA are higher than for China, despite China having lower damage parameters. This follows because the global planner assigns a higher weight to the marginal consumption gains in the lower-income regions, which in this case is China. Additionally, the welfare losses in the USA are greater than in other regions with similar damage profiles and income levels, such as EUR, due to the USA's higher potential for low-cost mitigation.

USA	EUR	CAZ	JPN	NEU	CHA	REF	LAM	MEA	OAS	IND	SSA
-2.9%	-0.3%	-1.6%	-0.7%	0.5%	-1.1%	-0.1%	1.1%	1.8%	2.4%	3.4%	4.0%

Table 3: Consumption equivalent (2015-2100 average) impacts of coordination

4.1.2 Emission reduction decomposition

In Figure 1, emissions in the coordination scenario decrease in comparison with the uncoordinated scenario. In this section, we quantify the channels of this reduction in emissions. The decomposition is undertaken in 4 steps. At every step we use a "shift-share" method to decompose an aggregate effect into two underlying channels. Consider a variable A that is the product of two other variables B and C, $A = BC$. Then the difference between two different states of A, i.e. $A_2 - A_1 = \Delta A = B_2C_2 - B_1C_1$, can be written as $\Delta A = \Delta BC_1 + B_1\Delta C + \Delta B\Delta C$, with $\Delta B = B_2 - B_1$ and $\Delta C = C_2 - C_1$. This formulation allows us to express ΔA as the sum of 3 terms, the first two of which, ΔBC_1 and $B_1\Delta C$, can be interpreted as the parts of ΔA that can be attributed to the change of one underlying variable if the other was held constant. To figure out if a change in B or a change in C contributed more to a change in A, a comparison of $\frac{\Delta BC_1}{\Delta A}$ with $\frac{B_1\Delta C}{\Delta A}$ would provide a good approximation, as long as $\Delta B\Delta C$ is small.

With this method at hand, we can proceed to our four-step decomposition of the reduction in global emissions between the uncoordinated and coordinated scenarios.

1. In the first step we decompose the reduction in global emissions into a reduction of global production and a reduction of global emission intensity of production[18].

2. In the second step we decompose the reduction of global emission intensity into a production shift from regions with high emission intensity to regions with low emission intensity and a reduction of regional emission intensities.

3. In the third - and for us most interesting - step we decompose the reduction of regional emission intensities into a production shift from sectors with high emission intensities to sectors with low emission intensities and a reduction of sectoral emission intensities.

4. In the fourth and final step we decompose the reduction of sectoral emission intensities of production into a reduction of energy use (in favor of labor and capital) and reduction of the emission intensity of sectoral energy.

For all steps, we perform the decomposition over 2015-2100 averaged results, i.e. we look at the differences between scenarios averaged over the entire model time-span.

Step 1: Figure 1 makes it clear, that global emissions are lower in the coordinated scenario than in the uncoordinated scenario. The results also show that global production decreases by about 8% and global emission intensity decreases by about 18%. The fact that the coordinated scenario has higher welfare even though production decreases is due to the internalization of the climate externality. The channel decomposition shows that approximately 30% of the reduction in global emissions is due to a reduction in global production, and 70% is due to a reduction in global emission intensity. The high share of the global emission intensity channel motivates its decomposition in step 2.

[18] In the following, if not otherwise specified, emission intensities always refer to emission intensities of production, i.e. emissions over output.

Step 2: Between the coordinated and uncoordinated solutions a slight shifting of regional production shares (as a share of global production) takes place. In Table 4 we see that in general, the production shares of high-income regions decrease, while the production shares of low-income regions increase. The production share of the United States for example decreases by 1.3 percentage points while that of Sub-Saharan Africa increases by 1 percentage point. This is due to the higher marginal utility of consumption and generally lower emission intensities in low-income regions,. A counterbalancing effect can be seen in the relatively low decrease, or even slight increase, in the production shares of the EU and Non-EU regions, high-income regions with low emission intensities, and the relatively low increase of India's production share a low income region with a relative high emission intensity.

USA	EUR	CAZ	JPN	NEU	CHA	REF	LAM	MEA	OAS	IND	SSA
-1.3%	-0.1%	-0.2%	-0.1%	0.1%	-0.7%	-0.2%	0.1%	0.3%	0.5%	0.6%	1.0%

Table 4: Change in production share (2015-2100 average) as share of global production between the coordinated and uncoordinated scenarios.

As for the emission intensities of production, they decrease in all regions, with larger reductions taking place in high-income regions than in low income regions, see Table 5. The channel decomposition shows that 1.5% of the reduction in global emission intensity is due to a shifting of regional production shares, and the 98.5% is due to a reduction in regional emission intensities. The high share of the regional emission intensity channel motivates its decomposition in step 3.

USA	EUR	CAZ	JPN	NEU	CHA	REF	LAM	MEA	OAS	IND	SSA
-27%	-22%	-32%	-25%	-14%	-28%	-20%	-14%	-18%	-8%	-13%	-8%

Table 5: Reduction in regional emission intensity of production (2015-2100 average) between the coordinated and uncoordinated scenarios.

Step 3: Across regions, we see that a shifting of sectoral production shares has taken place. Over the 2015-2100 period, all regions shift out of manufacturing and into services. This shift in production shares is mirrored by a shift in labor shares, see Figure 2. For most regions this shift is due to the fact that manufacturing is the most energy- and therefore emission- intensive sector. However in the case of the USA, thanks to a high sectoral energy productivity, the manufacturing sector is actually less energy and emission intensive than the service sector. The reason for which the USA nevertheless shifts out of manufacturing is because of an aggregate shift from investment to consumption within the region[19]. And since the aggregate consumption good requires more service goods then

[19]A reduction in investment leads to a decline in growth and future production, which decreases

the aggregate investment good, a shift from manufacturing towards services takes place.

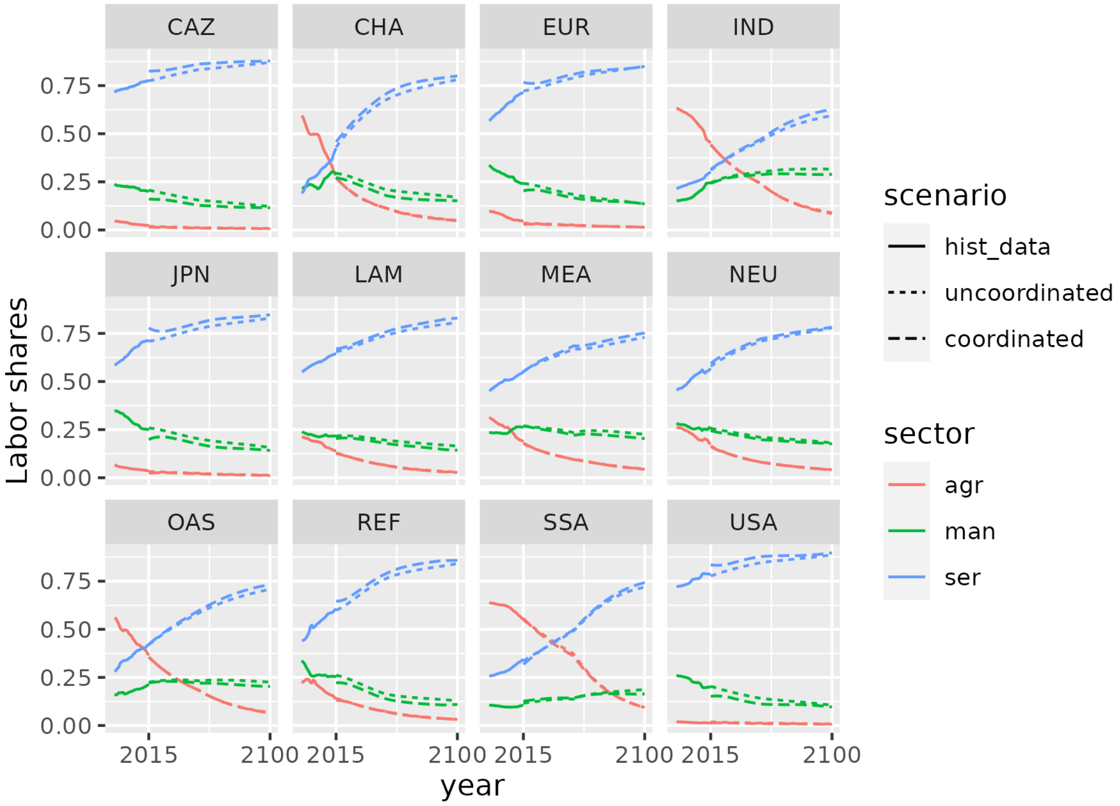

Figure 2: Labor shares over time.

Note: Figure 2 shows the labor shares over time for the coordinated and uncoordinated scenarios. Historical labor shares (from the World Bank's WDI) are shown under the scenario name "hist_data".

Another interesting point is that while it is true that all regions shift out of manufacturing in the long run, that is not the case in the short term. Figure 3 shows the difference in labor shares between the coordinated and uncoordinated scenarios averaged the 2015-2050 time span, and we see that SSA actually increases its share in manufacturing. This can be explained by the short-term increase in investments required in SSA to increase consumption in the long-term, and the fact that investments are manufacturing intensive.

As for the sectoral emission intensities, across regions and sectors they all decrease. For most regions the decrease in relative terms is smallest in the manufacturing sector, i.e. the sector where the elasticity between energy types is the smallest and thus the sector that is most difficult to decarbonize (see Appendix A.5 for a sensitivity analysis of the energy elasticity in the manufacturing sector.).

The decomposition shows that between 1.5% and 37% of the reduction in regional

emissions and therefore damages. This links back to the reduction of global production (only possible through a reduction of regional production, which itself is only possible if the factors of production decrease or are shifted to less efficient sectors) seen in Step 1.

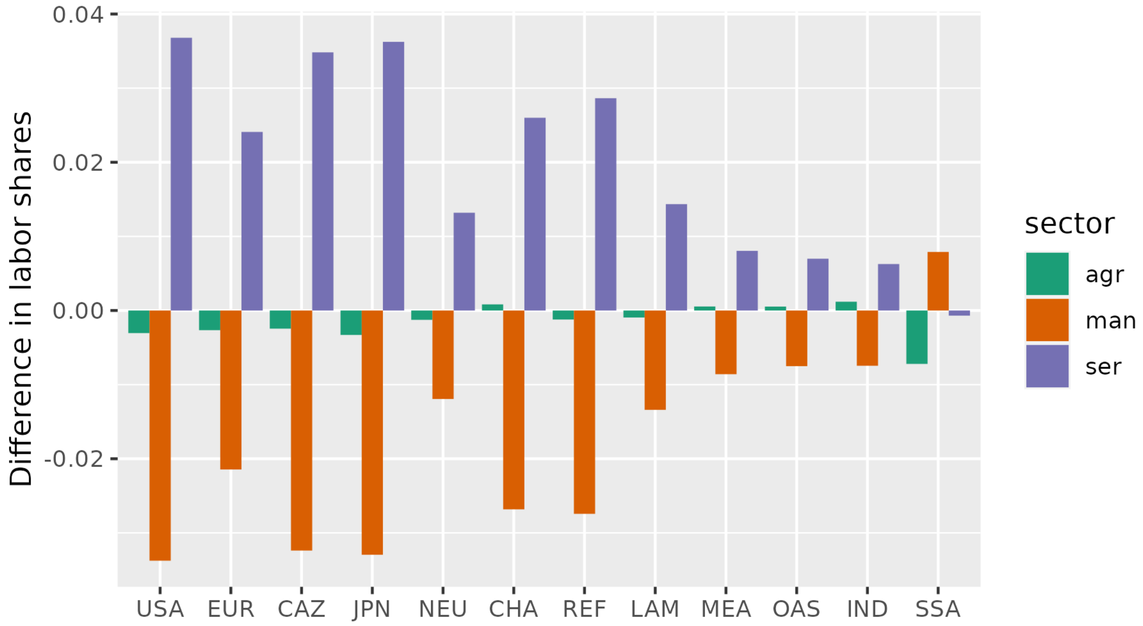

Figure 3: Change in labor allocation due to global coordination.

Note: Figure 3 shows the differences in labor shares averaged over the 2015-2050 time span between the coordinated and uncoordinated scenarios. The y-axis is in percentage points.

emission intensity is due to the shifting of economic activity between sectors, and between 63% and 95% of it is due to a decrease in sectoral emission intensities. Note the large variance of the channel importance across regions. The regions in which sectoral reallocation contributes most to the reduction in regional emission intensity are OAS, IND, CHA and REF. The regions in which sectoral reallocation contributes the least are EUR, SSA, USA and NEU. A key constraint of the sectoral reallocation channel is the complementarity of the sectoral goods in the aggregate consumption and investment functions (see Table 1).

Figure 4 illustrates the contributions of each sector to the two channels of regional emission intensity reduction. Looking closely, one can confirm that for all regions except USA, the positive contribution of the shift into services (positive contribution signifies that the channel increases regional emission intensity) is offset by the negative contribution of the shift out of manufacturing (compare the red bars).

In most regions, the reduction in sectoral emissions intensity is largest in the services sector. Energy sources are substitutes and easier to adjust in this sector than in the manufacturing sector where energy sources are complements. However, there are large differences across the regions for both the shift as well the share mechanism. Those regions that use the sectoral reallocation most to reduce emission intensity are also those that feature larger intensity reduction rates in the manufacturing sector. Because of a much larger initial emission intensity of the manufacturing sector compared to the service

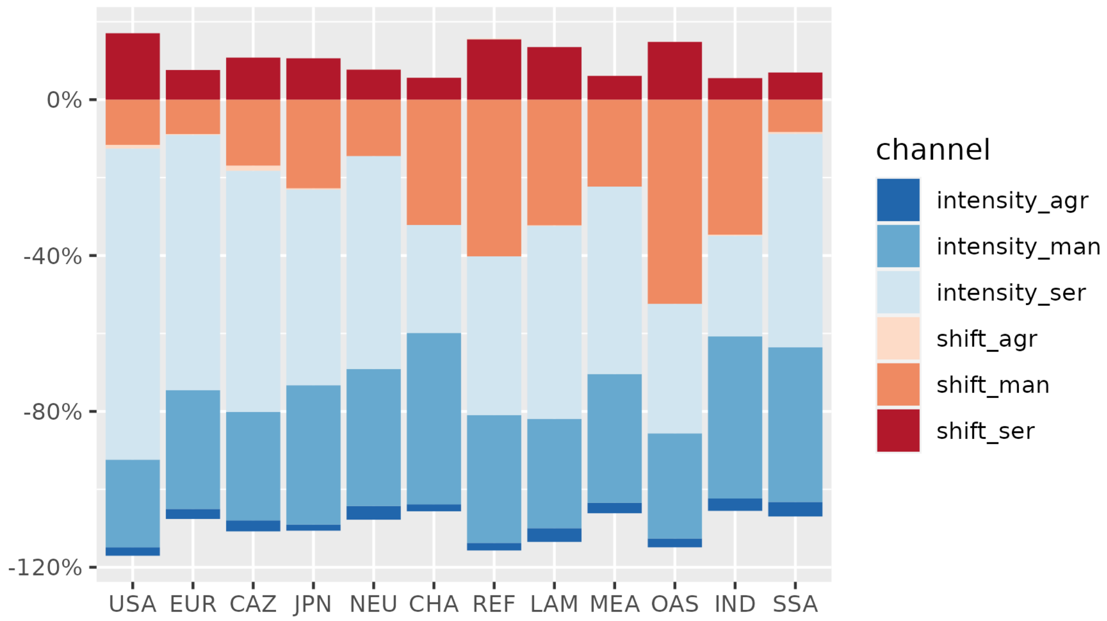

Figure 4: Decomposition of the reduction in regional emission intensities.

Note: Figure (4) shows the contribution of different channels in the reduction of the regional emission intensities as percentage of the total reduction in regional emission intensities. The different channels are the shift of sector allocations (shown in red colors) and the reduction in sector emission intensities (shown in blue colors). The contribution of each sector to the different channels are made clear by the shading. The contributions are calculated as averages over the 2015-2100 time-span. A negative contribution signifies that that channel contributes to a decrease in regional emission intensity. A positive value signifies the opposite.

sector, China, India and OAS can effectively reduce emission intensities by both moving out the of manufacturing sector and simultaneously decarbonizing it. The pattern is different in particular in USA, where in contrast to most other regions the service sector is more emission-intensive than the manufacturing sector.

Step 4: In every sector in every region, we see that coordination leads to less use of energy in favor of capital and labor. This shifting of production factors is constrained by the complementarity of the production factors, but takes place nonetheless. The sectoral emission intensity of energy decreases for most regions and sectors, however there are certain regions (IND, REF and OAS) in which every sector actually increases their emission intensity. For a sector to do this, i.e. shift energy demand from the low-emission energy type to the high-emission energy type, the high-emission energy type must either be much cheaper (to compensate for the incurred damages) or certain previously binding constraints stemming from the high damages experienced in the uncoordinated model must have become relaxed. The decomposition shows that for most regions and sectors the shifting of production factors in favor of capital and labor is the dominant channel in the reduction of the sectoral emission intensity of production, with only a few sectors in which the reduction of sectoral emission intensity of energy plays an important role, see

Figure 5.

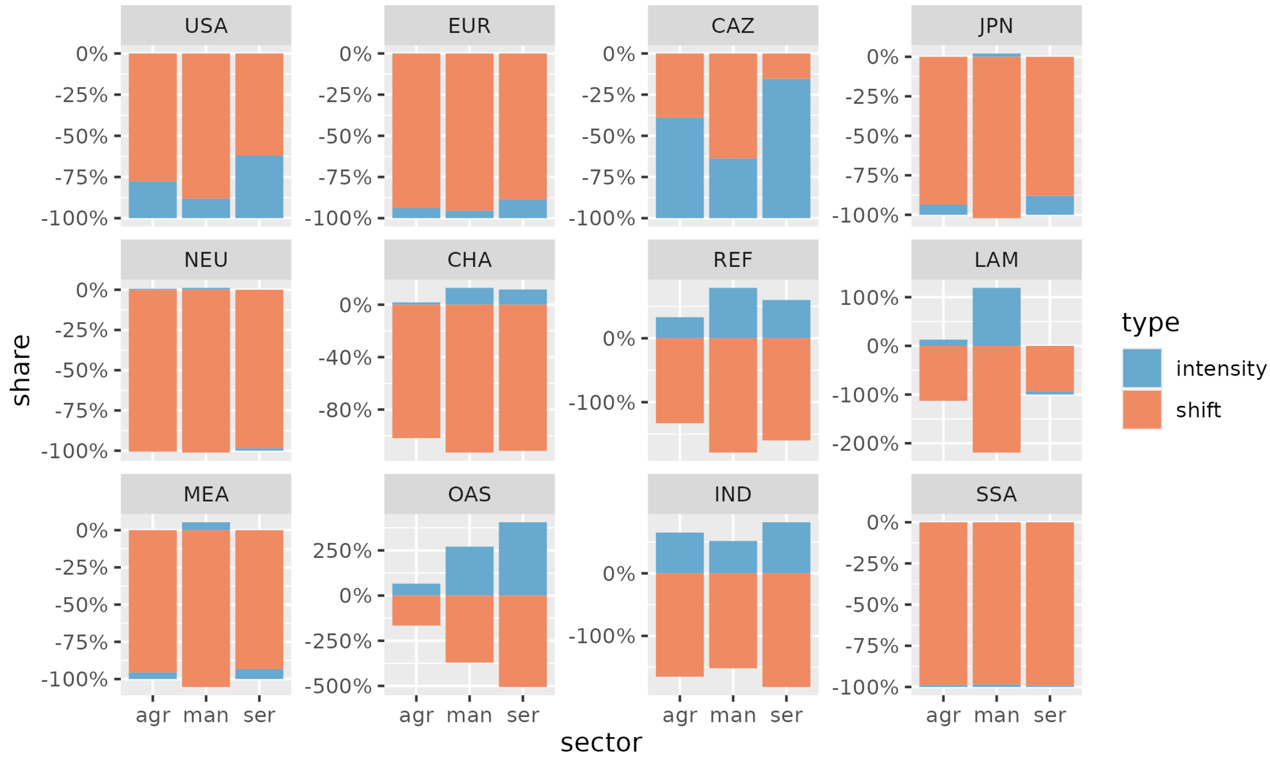

Figure 5: Decomposition of the reduction in sectoral emission intensities.

Note: Figure (5) shows the contribution of different channels in the reduction of the sectoral emission intensities of production, as percentage of the total reduction in sectoral emission intensities. The different channels are the shift of production factors (shown in red) and the shift in sector emission intensities of energy (shown in blue). The contributions are calculated as averages over the 2015-2100 time-span. A negative contribution signifies that that channel contributes to a decrease in sectoral emission intensity. A positive value signifies the opposite.

4.2 Higher damages

The structural change dynamics exhibited by the model in response to damages from climate change hinge on the parameters of the damage function (see Equation 11), which are inherently difficult to estimate. Nevertheless, they are the key components linking the economy and climate systems in most IAMs. We performed a sensitivity analysis of the damage function and find that an increase in damages leads to a drop in energy use and emissions for all regions and sectors, as expected. Noteworthy however is the fact that the changes in sector allocations vary across regions. Figure 6 shows the difference in labor shares between a coordination run with increased damages (50% increase across all regions and sectors) and one with default damages. While in developed regions higher damages lead to a shift of labor out of agriculture and manufacturing and into services, in developing regions, where agricultural production is closer to the subsistence level, higher damages cause labor to shift back into agriculture. In other words, we observe an asymmetric response to increases in climate damages across regions of different development status: the general pattern of structural change is furthered in developed regions, while it is hindered in developing regions. This means that if the damages from climate change turn out to be higher than expected, developing regions will be hindered that much further in their development.

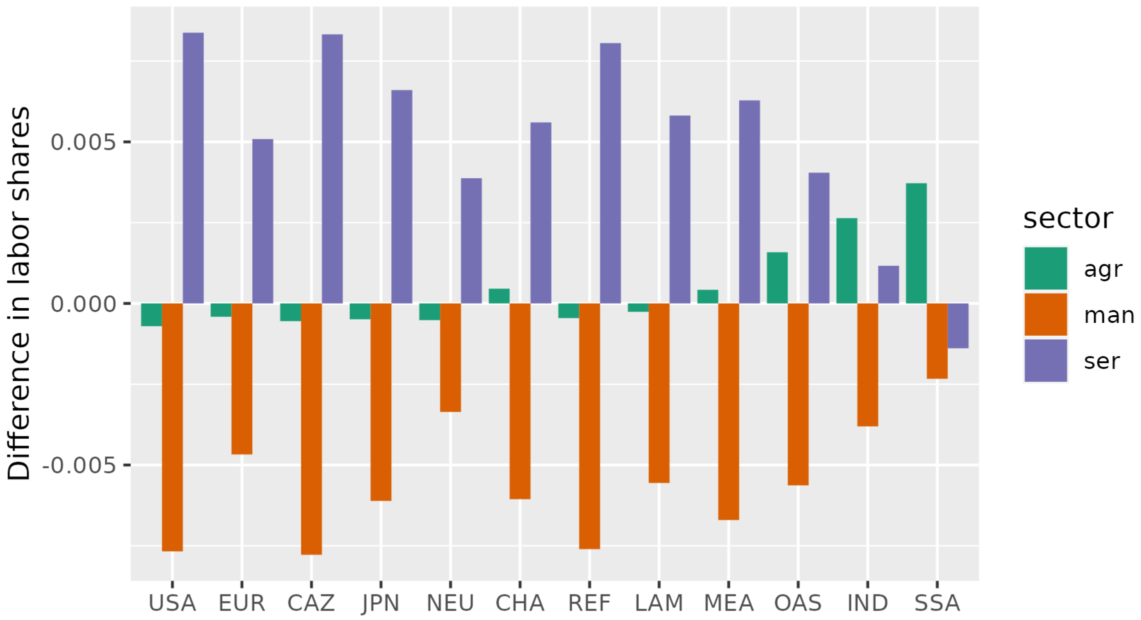

Figure 6: Change in labor allocation due to higher climate change damages.

Note: Figure 6 shows the differences in labor shares averaged over the 2015-2100 time span between the impact and coordinated scenarios. The y-axis is in percentage points.

4.3 Decarbonization of the energy system

In its current state, the model is limited in representing mitigation options. Thus, it is not able to trade consumption today for investments that would reduce damages and increase consumption in the future. However, one way in which the current model is able to recreate a climate mitigation scenario is to use energy prices and CO_2 intensities that correspond to a decarbonized energy system. In this case we use energy supply functions and carbon supply curves (see Appendix ...) derived from a REMIND 2°C warming scenario. The energy prices are higher in the mitigation scenario than in the coordination scenario, but the CO_2 intensities are lower. How do these differences affect the sector allocations?

As Figure 1 has shown, emissions decrease sharply in the mitigation scenario, dropping almost to 0 by 2070. This comes with a significant increase in energy expenditures and a reduction in the difference between emission intensities of the different energy types:

they all tend to zero over time. A consequence of this is that sectors are not hampered anymore by having to use an inefficient energy type only because of its lower emission intensity. The manufacturing sector, which is the most energy intensive sector in most regions, benefits the most from this, and thereby sees its share increase compared to the coordination scenario. Figure 7 illustrates this increase.

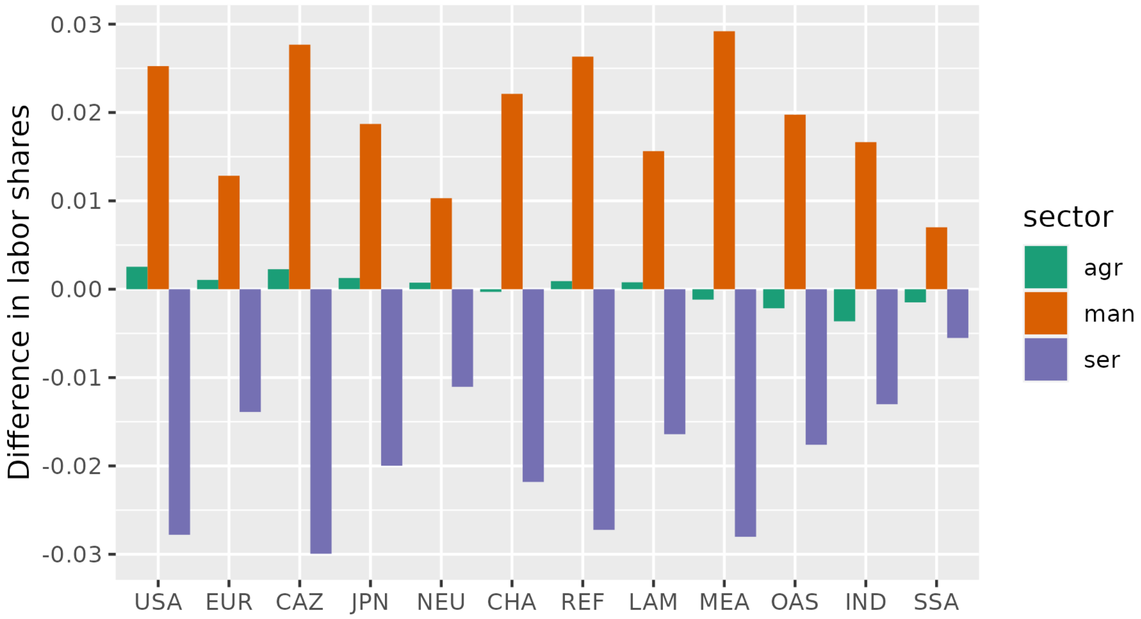

Figure 7: Change in labor allocation due to the decarbonization of the energy system.

Note: Figure 7 shows the differences in labor shares averaged over the 2015-2100 time span between the mitigation and coordinated scenarios. The y-axis is in percentage points.

Noteworthy is the variation of the differences in the agricultural sector: for high-income regions, the mitigation scenario has a higher labor share in the agricultural sector than the coordination scenario, while for low-income regions it is the opposite. Like in the impact-coordination comparison, we observe an asymmetric response across regions with different development status, but this time a progressive one. In response to the decarbonization of the energy sector, the general pattern of structural change is furthered in developing regions, while it is hindered in developed regions. This seems to indicate that implementing mitigation policies should have a positive effect on the structural composition of developing economies.

5 Conclusion

References

Allen, M. R. (2016). Drivers of peak warming in a consumption-maximizing world. *Nature Climate Change*, 6(7):684–686.

Baccianti, C. (2013). Estimation of Sectoral Elasticities of Substitution Along the International Technology Frontier. *SSRN Electronic Journal*.

Bah, E. H. M. and Brada, J. C. (2009). Total factor productivity growth, structural change and convergence in the new members of the European Union. *Comparative Economic Studies*, 51(4):421–446.

Baumstark, L., Bauer, N., Benke, F., Bertram, C., Bi, S., Gong, C. C., Dietrich, J. P., Dirnaichner, A., Giannousakis, A., Hilaire, J., Klein, D., Koch, J., Leimbach, M., Levesque, A., Madeddu, S., Malik, A., Merfort, A., Merfort, L., Odenweller, A., Pehl, M., Pietzcker, R. C., Piontek, F., Rauner, S., Rodrigues, R., Rottoli, M., Schreyer, F., Schultes, A., Soergel, B., Soergel, D., Strefler, J., Ueckerdt, F., Kriegler, E., and Luderer, G. (2021). REMIND2.1: Transformation and innovation dynamics of the energy-economic system within climate and sustainability limits. *Geoscientific Model Development Discussions*, pages 1–50. Publisher: Copernicus GmbH.

Buiatti, C., Duarte, J., and Saenz, F. (2017). Why Is Europe Falling Behind? Structural Transformation and Services' Productivity Differences between Europe and the U.S.

Ciarli, T. and Savona, M. (2019). Modelling the Evolution of Economic Structure and Climate Change: A Review. *Ecological Economics*, 158:51–64.

Collins, M., Knutti, R., Arblaster, J., Dufresne, J.-L., Fichefet, T., Friedlingstein, P., Gao, X., Gutowski, W. J., Johns, T., Krinner, G., Shongwe, M., Tebaldi, C., Weaver, A. J., and Wehner, M. (2013). Chapter 12 - Long-term climate change: Projections, commitments and irreversibility. In IPCC, editor, *Climate Change 2013: The Physical Science Basis. IPCC Working Group I Contribution to AR5*. Cambridge University Press, Cambridge.

Comin, D., Lashkari, D., and Mestieri, M. (2021). Structural Change With Long-Run Income and Price Effects. *Econometrica*, 89(1):311–374. _eprint: https://onlinelibrary.wiley.com/doi/pdf/10.3982/ECTA16317.

Dellink, R., Chateau, J., Lanzi, E., and Magné, B. (2017). Long-term economic growth projections in the Shared Socioeconomic Pathways. *Global Environmental Change*, 42:200–214.

Dietz, S. and Venmans, F. (2019). Cumulative carbon emissions and economic policy: In search of general principles. *Journal of Environmental Economics and Management*, 96:108–129.

Duarte, M. and Restuccia, D. (2010). The role of the structural transformation in aggregate productivity. *Quarterly Journal of Economics*, 125(1):129–173.

Fávero, L. P., Souza, R. D. F., Belfiore, P., Luppe, M. R., and Severo, M. (2022). Global relationship between economic growth and CO<SUB align="right">2 emissions across time: a multilevel approach. *International Journal of Global Warming*, 26(1):38.

García-Santana, M., Pijoan-Mas, J., and Villacorta, L. (2021). Investment Demand and Structural Change. *Econometrica*, 89(6):2751–2785. _eprint: https://onlinelibrary.wiley.com/doi/pdf/10.3982/ECTA16295.

Golosov, M. (2014). Optimal Taxes on Fossil Fuel in General Equilibrium. *Econometrica*, 82(1):41–88.

Herrendorf, B., Rogerson, R., and Valentinyi, A. (2013). Two Perspectives on Preferences and Structural Transformation. *American Economic Review*, 103(7):2752–2789.

Herrendorf, B., Rogerson, R., and Valentinyi, A. (2014). Growth and Structural Transformation. In *Handbook of Economic Growth*, volume 2, pages 855–941. Elsevier.

IPCC, editor (2024). *Climate Change 2022 - Mitigation of Climate Change: Working Group III Contribution to the Sixth Assessment Report of the Intergovernmental Panel on Climate Change*. Cambridge University Press, Cambridge. DOI:.

Koch, J. and Leimbach, M. (2023). SSP economic growth projections: Major changes of key drivers in integrated assessment modelling. *Ecological Economics*, 206:107751.

Lefèvre, J., Le Gallic, T., Fragkos, P., Mercure, J.-F., Simsek, Y., and Paroussos, L. (2022). Global socio-economic and climate change mitigation scenarios through the lens of structural change. *Global Environmental Change*, 74:102510.

Leimbach, M., Marcolino, M., and Koch, J. (2023). Structural change scenarios within the SSP framework.

MacDougall, A. H. (2016). The Transient Response to Cumulative CO2 Emissions: a Review. *Current Climate Change Reports*, 2(1):39–47.

Maddison, A. (1980). Economic Growth and Structural Change in Advanced Countries. In *Western Economies in Transition: Structural Change and Adjustment Policies in Industrial Countries*. Croom Helm.

Madeddu, S., Ueckerdt, F., Pehl, M., Peterseim, J., Lord, M., Kumar, K. A., Krüger, C., and Luderer, G. (2020). The CO_2 reduction potential for the European industry via direct electrification of heat supply (power-to-heat). *Environmental Research Letters.*

Matthews, H. D., Gillett, N. P., Stott, P. A., and Zickfeld, K. (2009). The proportionality of global warming to cumulative carbon emissions. *Nature*, 459(7248):829–832.

Moro, A., Moslehi, S., and Tanaka, S. (2017). Does home production drive structural transformation? *American Economic Journal: Macroeconomics*, 9(3):116–146.

Nordhaus, W. (1992a). The 'Dice' Model: Background and Structure of a Dynamic Integrated Climate-Economy Model of the Economics of Global Warming. *Cowles Foundation Discussion Papers.*

Nordhaus, W. D. (1992b). An Optimal Transition Path for Controlling Greenhouse Gases. *Science*, 258(5086):1315–1319.

Nordhaus, W. D. and Yang, Z. (1996). A Regional Dynamic General-Equilibrium Model of Alternative Climate-Change Strategies. *American Economic Review*, 86(4):741–765.

Parrado, R. and de Cian, E. (2014). Technology spillovers embodied in international trade: Intertemporal, regional and sectoral effects in a global CGE framework. *Energy Economics*, 41:76–89.

Riahi, K., van Vuuren, D. P., Kriegler, E., Edmonds, J., O'Neill, B. C., Fujimori, S., Bauer, N., Calvin, K., Dellink, R., Fricko, O., Lutz, W., Popp, A., Cuaresma, J. C., Kc, S., Leimbach, M., Jiang, L., Kram, T., Rao, S., Emmerling, J., Ebi, K., Hasegawa, T., Havlik, P., Humpenöder, F., Da Silva, L. A., Smith, S., Stehfest, E., Bosetti, V., Eom, J., Gernaat, D., Masui, T., Rogelj, J., Strefler, J., Drouet, L., Krey, V., Luderer, G., Harmsen, M., Takahashi, K., Baumstark, L., Doelman, J. C., Kainuma, M., Klimont, Z., Marangoni, G., Lotze-Campen, H., Obersteiner, M., Tabeau, A., and Tavoni, M. (2017). The Shared Socioeconomic Pathways and their energy, land use, and greenhouse gas emissions implications: An overview. *Global Environmental Change*, 42:153–168.

Schultz, T. W. (1953). *The Economic Organization of Agriculture.* McGraw-Hill, New York.

Stefanski, R. (2014). Structural transformation and the oil price. *Review of Economic Dynamics*, 17(3):484–504.

Stern, D. I. (2012). Interfuel Substitution: A Meta-Analysis. *Journal of Economic Surveys*, 26(2):307–331. _eprint: https://onlinelibrary.wiley.com/doi/pdf/10.1111/j.1467-6419.2010.00646.x.

van der Wijs, K.-I., Bosello, F., Dasgupta, S., Drouet, L., Emmerling, J., Hof, A., Leimbach, M., Parrado, R., Piontek, F., Standardi, G., and van Vuuren, D. (2022). New damage curves and nulti-model analysis suggest lower optimal temperature. *Nature Climate Change, under review.*

Üngör, M. (2017). Productivity growth and labor reallocation: Latin America versus East Asia. *Review of Economic Dynamics*, 24:25–42.

Świecki, T. (2017). Determinants of structural change. *Review of Economic Dynamics*, 24:95–131.

A Appendix

A.1 Variations of the benchmark model

A.1.1 Single energy type

In this version of the model, we assume only a single energy type, in other words we don't distinguish between electric and non-electric final energy demand, and instead only have "total" final energy demand $e_{it}^{tot} = e_{it}$. This means that we can essentially drop Equation 4 and use slight variations for Equations 7 and 9:

$$c_{it} + x_{it} = y_{it} - \psi_{it}^{tot} e_{it}^{tot} \tag{14}$$

$$emi_t = \sum_{i \in \{a,m,s\}} \xi_t^{tot} e_{it}^{tot} \tag{15}$$

where ψ_{it}^{tot} and ξ_t^{tot} are the opportunity cost of total final energy in terms of good i, and the CO2 intensity of total final energy, respectively. The rest of the model stays as it is in the benchmark, see Section 2.

A.1.2 Competitive equilibrium formulation

The competitive equilibrium discusses how the different economic agents (households and firms) interact in markets. Assumptions on the market structure and ownership of factors of production are necessary to characterize the final allocation and the prices of the economy. We assume that a representative household owns the factors of production, rents them to firms and supplies one unit of labor inelastically. Firms are competitive at both input and output markets, and capital is the numeraire. We use the same notation as in our benchmark model, with the addition of the wage rate w_t, capital rent r_t, and the hat notation $\hat{x}$ to indicate equilibrium.

A competitive equilibrium is prices $\{(\hat{p}_{it})_{i\in\{a,m,s\}}, \hat{w}_t, \hat{r}_t, \hat{p}_t^{el}, \hat{p}_t^{noel}\}_{t=0}^{\infty}$, household allocation $\{(\hat{c}_{it}, \hat{x}_{it})_{i\in\{a,m,s\}}, \hat{k}_{t+1}, \hat{e}_t^{el}, \hat{e}_t^{noel}\}_{t=0}^{\infty}$, firms' allocation $\{(\hat{k}_{it}^d, \hat{l}_{it}^d, \hat{e}_t^{d,el}, \hat{e}_t^{d,noel})_{i\in\{a,m,s\}}\}_{t=0}^{\infty}$, and investment firm's allocation $\{(\hat{x}_{it}^d)_{i\in\{a,m,s\}}\}_{t=0}^{\infty}$ s.t.:

1. Given $\{\hat{p}_{it}, \hat{w}_t, \hat{r}_t, \hat{p}_t^{el}, \hat{p}_t^{noel}\}$, household allocation solves:

$$\begin{aligned} &\max \sum_{t=0}^{\infty} \beta^t \ln(c_t) \\ &\text{s.t.} \sum_{i\in\{a,m,s\}} \hat{p}_{it}(c_{it} + x_{it} + \hat{\psi}_{it}^{el} e_{it}^{el} + \hat{\psi}_{it}^{noel} e_{it}^{noel}) = \hat{w}_t + \hat{r}_t k_t + \hat{p}_t^{el} e_t^{el} + \hat{p}_t^{noel} e_t^{noel} \\ &\quad k_{t+1} = (1-\delta)k_t + x_t \end{aligned} \tag{16}$$

2. Given $\{\hat{p}_{it}, \hat{w}_t, \hat{r}_t, \hat{p}_t^{el}, \hat{p}_t^{noel}\}$, the allocation of each firm of sectors $i \in \{a, m, s\}$ solves its maximization problem:

$$\max \hat{p}_{it} y_{it} - \hat{w}_t l_{it}^d - \hat{r}_t k_{it}^d - \hat{p}_t^{el} e_{it}^{el,d} - \hat{p}_t^{noel} e_{it}^{noel,d} \tag{17}$$

3. Given $\{\hat{p}_{it}\}$, the investment firm's allocation solves its maximization problem:

$$\max A_{xt} \left[\sum_{i \in \{a,m,s\}} (\theta_i^x)^{\frac{1}{\nu_x}} x_{it}^{d\,\frac{\nu_x - 1}{\nu_x}} \right]^{\frac{\nu_x}{\nu_x - 1}} - \sum_{i \in \{a,m,s\}} \hat{p}_{it} x_{it}^d \tag{18}$$

4. Markets clear:

$$\begin{aligned} \hat{c}_{it} + \hat{x}_{it} + \hat{\psi}_{it}^{el} e_{it}^{el} + \hat{\psi}_{it}^{noel} e_{it}^{noel} &= \hat{y}_{it}, \quad i \in \{a, m, s\} \\ \hat{k}_t &= \sum_{i \in \{a,m,s\}} \hat{k}_{it}^d \\ 1 &= \sum_{i \in \{a,m,s\}} \hat{l}_{it}^d \\ \hat{e}_t^{el} &= \sum_{i \in \{a,m,s\}} \hat{e}_{it}^{el,d} \\ \hat{e}_t^{noel} &= \sum_{i \in \{a,m,s\}} \hat{e}_{it}^{noel,d} \end{aligned} \tag{19}$$

A.2 Calibration of productivities

To calibrate the productivities of our model, we set targets and adjust the productivities' start-year levels and growth rates until the model allocation matches these targets. The start-year of our model is always a historic year, whereas the end-year may lie in the future.

A.2.1 Start-year levels

The targets for the productivities' start-year levels, are historic data on GDP, investment to GDP ratios, and sectoral labor and energy allocations.

Data on GDP and employment shares is sourced from World Bank's World Development Indicators (WDI) database. We use the series "NY.GDP.MKTP.PP.KD" (GDP, PPP (constant 2017 international $)) for GDP, and the series "SL.AGR.EMPL.ZS", "SL.AGR.EMPL.ZS", and "SL.AGR.EMPL.ZS" for employment shares in the agriculture, manufacturing and services sectors, respectively.

Data for the share of investment relative to GDP is from the Penn World Tables (PWT) 9.1. We use the variable "csh_i".

The energy data is from the International Energy Agency (IEA) Energy Balances database. We use the IEA product "Total" for final energy in ktoe. We consider as energy use in the agriculture sector the IEA "flows" Agriculture/Forestry (AGRICULT) and Fishing (FISHING). Manufacturing energy use is Industry (TOTIND), Non-energy use industry (NEINTREN), and Energy Industry Own Use and Losses (TOTENGY). Services energy use is Transport (TOTTRANS), Residential (RESIDENT), Commercial and Public Services (COMMPUB), Non-Specified (ONONSPEC), Non-energy use in transport (NETRANS) and Non-energy use in other (NEOTHER).

A.2.2 Growth rates

To pin down the sectoral productivity growth rates (we assume steady growth over time), we use a set of aggregate and sectoral targets on GDP, capital, labor and energy. If the end-year of the model is in the past, the targets are from the same databases as for the start-year levels. If the end-year is in the future, then the targets are taken from SSP projections: see Koch and Leimbach (2023) for GDP projections, REMIND (Baumstark et al. (2021)) for energy levels, and Leimbach et al. (2023) for sectoral labor and energy shares[20]. For the labor and energy share targets, we allow for some flexibility by constructing brackets (essentially a target range, bounded by a largest and smallest accepted value) in the end year based on the predictions from Leimbach et al. (2023). The intervals are centered on the prediction value, with an upper bound 2.5% above the prediction, and the lower bound 2.5% below. For example, the prediction for agricultural employment share in India in 2050 is 23%. Therefore, the bracket in 2050 for l_a would range from 20.5% to 25.5%.

A.2.3 Type-specific energy productivities

To compute the specific energy productivities B_{it}^{el} and B_{it}^{noel} we make the assumption that the energy composite e_{it} is the same in both the 1-energy and 2-energy formulations of our models. Using the price information from REMIND and the energy targets, we can then pin down the productivities. Need to rewrite this section.

Consider the problem of maximizing e_{it} given energy prices:

$$\max \left[(\theta_i^e)^{1-\rho_i^e} \left(B_{it}^{noel} e_{it}^{noel} \right)^{\rho_i^e} + (1-\theta_i^e)^{1-\rho_i^e} \left(B_{it}^{el} e_{it}^{el} \right)^{\rho_i^e} \right]^{\frac{1}{\rho_i^e}} - p_t^{noel} e_{it}^{noel} - p_t^{el} e_{it}^{el} \qquad (20)$$

[20]Leimbach et al. (2023) provides predictions of total sectoral final energy, not of electric and non-electric final energy, but we use the same method to construct predictions for electric and non-electric final energy.

where $\rho_i^e = \frac{\nu_i^e}{\nu_i^e - 1}$. The first order conditions are:

$$\begin{aligned} &\min p_t^{noel} e_{it}^{noel} + p_t^{el} e_{it}^{el} \\ &s.t. \left[(\theta_i^e)^{1-\rho_i^e} \left(B_{it}^{noel} e_{it}^{noel} \right)^{\rho_i^e} + (1-\theta_i^e)^{1-\rho_i^e} \left(B_{it}^{el} e_{it}^{el} \right)^{\rho_i^e} \right]^{\frac{1}{\rho_i^e}} = \bar{e}_{it} \end{aligned} \tag{21}$$

$$\begin{aligned} \frac{\partial}{\partial e_{it}^{noel}} &: \frac{1}{\rho_i^e} [.]^{\frac{1}{\rho_i^e}-1} (\theta_i^e)^{1-\rho_i^e} \rho_i^e \left(B_{it}^{noel} e_{it}^{noel} \right)^{\rho_i^e - 1} B_{it}^{noel} - p_t^{noel} = 0 \\ \frac{\partial}{\partial e_{it}^{el}} &: \frac{1}{\rho_i^e} [.]^{\frac{1}{\rho_i^e}-1} (1-\theta_i^e)^{1-\rho_i^e} \rho_i^e \left(B_{it}^{el} e_{it}^{el} \right)^{\rho_i^e - 1} B_{it}^{el} - p_t^{el} = 0 \end{aligned} \tag{22}$$

Rearranging, we get:

$$\begin{aligned} [.]^{\frac{1}{\rho_i^e}-1} (\theta_i^e)^{1-\rho_i^e} \left(B_{it}^{noel} e_{it}^{noel} \right)^{\rho_i^e} &= p_t^{noel} e_{it}^{noel} \\ [.]^{\frac{1}{\rho_i^e}-1} (1-\theta_i^e)^{1-\rho_i^e} \left(B_{it}^{el} e_{it}^{el} \right)^{\rho_i^e} &= p_t^{el} e_{it}^{el} \end{aligned} \tag{23}$$

then:

$$\begin{aligned} [.]^{\frac{1}{\rho_i^e}-1} (\theta_i^e)^{1-\rho_i^e} \left(B_{it}^{noel} \right)^{\rho_i^e} \frac{1}{p_t^{noel}} &= (e_{it}^{noel})^{1-\rho_i^e} \\ [.]^{\frac{1}{\rho_i^e}-1} (1-\theta_i^e)^{1-\rho_i^e} \left(B_{it}^{el} \right)^{\rho_i^e} \frac{1}{p_t^{el}} &= (e_{it}^{el})^{1-\rho_i^e} \end{aligned} \tag{24}$$

and finally:

$$\begin{aligned} e_{it}^{noel} &= [.]^{\frac{1}{\rho_i^e}} \theta_i^e \left(B_{it}^{noel} \right)^{\frac{\rho_i^e}{1-\rho_i^e}} \frac{1}{(p_t^{noel})^{\frac{1}{1-\rho_i^e}}} \\ e_{it}^{el} &= [.]^{\frac{1}{\rho_i^e}} (1-\theta_i^e) \left(B_{it}^{el} \right)^{\frac{\rho_i^e}{1-\rho_i^e}} \frac{1}{(p_t^{el})^{\frac{1}{1-\rho_i^e}}} \end{aligned} \tag{25}$$

Dividing the equations, we get:

$$\frac{e_{it}^{noel}}{e_{it}^{el}} = \frac{\theta_i^e}{1-\theta_i^e} \left(\frac{p_i^{el}}{p_i^{noel}} \right)^{\frac{1}{1-\rho_i^e}} \left(\frac{B_{it}^{noel}}{B_{it}^{el}} \right)^{\frac{\rho_i^e}{1-\rho_i^e}} \tag{26}$$

or:

$$\frac{B_{it}^{noel}}{B_{it}^{el}} = \left(\frac{1-\theta_i^e}{\theta_i^e} \frac{e_{it}^{noel}}{e_{it}^{el}} \right)^{\frac{1-\rho_i^e}{\rho_i^e}} \left(\frac{p_i^{noel}}{p_i^{el}} \right)^{\frac{1}{\rho_i^e}} \tag{27}$$

Finally, we rewrite Equation 4 as follows:

$$e_{it} = B_{it}^{el} \left[\theta_i^{e\,\frac{1}{\nu_i^e}} \left(\frac{B_{it}^{noel}}{B_{it}^{el}} e_{it}^{noel} \right)^{\frac{\nu_i^e - 1}{\nu_i^e}} + (1-\theta_i^e)^{\frac{1}{\nu_i^e}} \left(e_{it}^{el} \right)^{\frac{\nu_i^e - 1}{\nu_i^e}} \right]^{\frac{\nu_i^e}{\nu_i^e - 1}} \tag{28}$$

With Equations 27 and 28, and given e_{it} (from the single energy type variation of the model), e^{el}_{it} and e^{noel}_{it} (from the start and end year targets), we can then pin down B^{el}_{it} and B^{noel}_{it}. The energy prices are known, since they are defined as part of the calibration, see A.3

A.3 Price of energy

The model does not consider energy supply explicitly. To introduce a costly energy demand, we set $\psi^{el}_{it} = p^{el}_t / p_{it}$ and $\psi^{noel}_{it} = p^{noel}_t / p_{it}$ (see 7), where p^{el}_t and p^{noel}_t are the energy prices and p_{it} are the sector prices relative to the numeraire, i.e. capital. The energy prices are constructed, and adjusted, using exogenous energy supply curves, and the sector prices are derived using the competitive equilibrium formulation of the model (see A.1.2).

A.3.1 Energy supply curves

We use energy supply curves consistent with REMIND (REgional Model of INvestment and Development) integrated assessment model. REMIND is a numerical model that represents the future evolution of the world economies with a special focus on the development of the energy sector (Baumstark et al. (2021)). We take advantage of its careful description of the energy system to construct linear energy price curves of the form:

$$
\begin{aligned}
p^{el}_{jt} &= m^{el}_{jt} + n^{el}_{jt} Q^{el}_{jt} \\
p^{noel}_{jt} &= m^{noel}_{jt} + n^{noel}_{jt} Q^{noel}_{jt}
\end{aligned} \tag{29}
$$

where m^{el}_{jt}, m^{noel}_{jt}, n^{el}_{jt} and n^{noel}_{jt} are the region-specific supply curve parameters, and Q^{el}_{jt} and Q^{noel}_{jt} are the quantities of the different energy types.

The supply curve parameters are also scenario specific. They are constructed from REMIND results, and are consistent with scenario assumptions that underpin these results, e.g. SSP scenario or mitigation level (baseline, 2°C stabilization).

A.3.2 Sector prices

To calculate the sectoral prices we take advantage of the Second Welfare Theorem. The prices of the sector goods are derived from the competitive equilibrium formulation of the model (see A.1.2), specifically the investment firm's maximization problem given by (Equation 18, repeated here for clarity):

$$
\max A_{xt} \left[\sum_{i \in \{a,m,s\}} (\theta^x_i)^{\frac{1}{\nu_x}} \, {x^d_{it}}^{\frac{\nu_x - 1}{\nu_x}} \right]^{\frac{\nu_x}{\nu_x - 1}} - \sum_{i \in \{a,m,s\}} \hat{p}_{it} x^d_{it} \tag{18}
$$

With $x_t = \left[\sum_{i\in\{a,m,s\}} (\theta_i^x)^{\frac{1}{\nu_x}} x_{it}^{d\ \frac{\nu_x-1}{\nu_x}}\right]$, the first order conditions for every sector can be written as:

$$\frac{\partial}{\partial x_{it}^d} : A_{xt} x_t^{\frac{1}{\nu_x-1}} (\theta_i^x)^{\frac{1}{\nu_x}} \left(x_{it}^d\right)^{\frac{\nu_x-1}{\nu_x}-1} - \hat{p}_{it} = 0 \tag{30}$$

and so:

$$\hat{p}_{it} = A_{xt} x_t^{\frac{1}{\nu_x-1}} (\theta_i^x)^{\frac{1}{\nu_x}} (x_{it})^{\frac{\nu_x-1}{\nu_x}-1} \tag{31}$$

A.3.3 Adjustment mechanism

To make sure that the energy demand (which in the model is given by $Q_t^{el} = \sum_{i\in\{a,m,s\}} e_{it}^{el}$ and $Q_t^{noel} = \sum_{i\in\{a,m,s\}} e_{it}^{noel}$) and energy prices implied by our model are consistent with the REMIND supply curves, we run the model multiple times and adjust ψ_{it}^{el} and ψ_{it}^{noel} between iterations, until the resulting energy demand and implied energy prices are consistent with 29.

A.4 CO2 intensity of energy

As with the price of energy, we rely on the REMIND model to provide us with future pathways of CO2 intensities of the different final energy types. In REMIND, depending on the amount of final energy demanded, the manner of production of said energy will vary, as the model decides how best to use all the different primary energy types and secondary transformation technologies available. For example, depending on if the next megawatt of electricity is best produced with or without fossil fuels, an increase of electricity demand in any given region and in any given year, can be associated with higher or lower carbon intensity. As a consequence, the CO2 intensities of final energies are time-dependent and region-specific. We compute the CO2 intensities ξ_{jt}^{el}, and ξ_{jt}^{noel} using the following carbon curves constructed from REMIND results:

$$\begin{aligned} emi_{jt}^{el} &= g_{jt}^{el} + h_{jt}^{el} Q_{jt}^{el} \\ emi_{jt}^{noel} &= g_{jt}^{noel} + h_{jt}^{noel} Q_{jt}^{noel} \end{aligned} \tag{32}$$

where g_{jt}^{el}, g_{jt}^{noel}, h_{jt}^{el} and h_{jt}^{noel} are region-specific carbon curve parameters, emi_{jt}^{el} and emi_{jt}^{noel} are the CO2 emissions, and Q_{jt}^{el} and Q_{jt}^{noel} are the quantities of the different energy types. As is the case with the energy supply curves parameters, the carbon curve parameters are also scenario specific. They are constructed from REMIND results, and are consistent with scenario assumptions that underpin these results, e.g. SSP scenario or mitigation level (baseline, 2°C stabilization). The CO2 intensities for our model are then computed as $\xi_{jt}^{el} = emi_{jt}^{el}/Q_{jt}^{el}$ and $\xi_{jt}^{noel} = emi_{jt}^{noel}/Q_{jt}^{noel}$, once again using $Q_t^{el} = \sum_{i\in\{a,m,s\}} e_{jit}^{el}$ and $Q_t^{noel} = \sum_{i\in\{a,m,s\}} e_{jit}^{noel}$.

The direct CO2 emissions from industrial processes and the CO2 emissions from land-use change emi_{jt}^{other} are also taken from the REMIND model and are scenario specific.

In the base SSP2 scenario they represent, in most regions, only a very small share of the total CO2 emissions. Sub-Saharan Africa is an exception in that CO2 emission from land-use change represents the a very large share of the total CO2 emissions, specifically in the early periods, see figure.

A.5 Sensitivity to the manufacturing energy elasticity

The structural change dynamics exhibited by the multi-sector growth model in response to damages from climate change hinge on key parameters, amongst which are the elasticities of substitution between final energy types (ν_i^e).

The differences that exist between sectors with regard to their elasticities of substitution between final energy types, means that when reacting to damages from CO2 emissions, some sectors are able to switch from a high-carbon energy type to a low-carbon energy type more easily than others. To better understand how the values of the elasticities influence the model's structural change dynamics, a sensitivity analysis was performed on the energy elasticity in the manufacturing sector, the single sector in which the energy types are complements by default. We find, as expected, that increasing the energy elasticity in the manufacturing sector and thereby facilitating the replacement of carbon intensive energy with cleaner energy, leads to a reduction in aggregate emissions, see Fig. 8. Varying the energy elasticity in manufacturing has a direct effect on the energy composition in the manufacturing sector. With high elasticities, changes in use of non-electric energy in the manufacturing sector vary between -35% and 30% across regions. Large differences across regions and time are due to region-specific evolution of specific costs and emission intensities linked to electricity and non-electricity energy use.

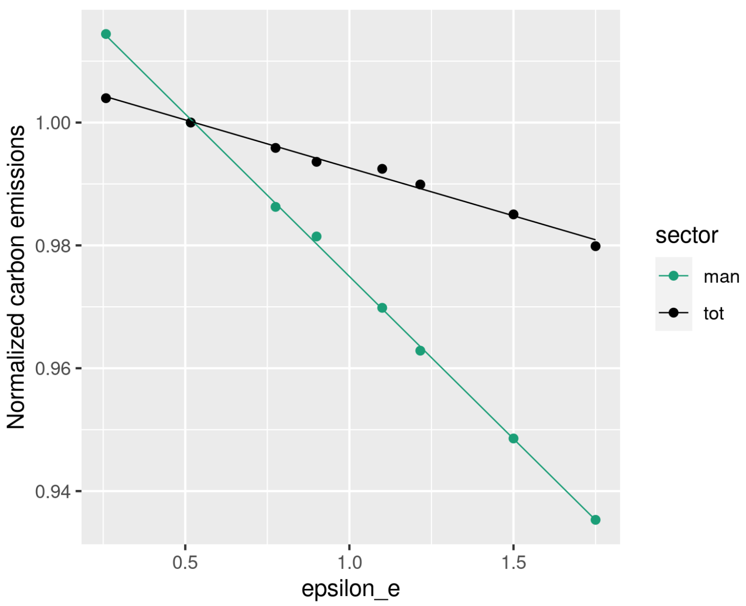

Figure 8: Sensitivity to energy elasticity in the manufacturing sector.

However, these sometimes large relative changes in energy composition do not translate to large differences in labor shares, see Fig. 9. So while the energy composition is very sensitive to a change in the energy elasticity, the overall sectoral composition in terms of labor allocations is not. Nevertheless, it is interesting to realize that as the energy elasticity in the manufacturing sector increases, so does the share of labor allocated to the manufacturing sector increase, as the model takes advantage of a less carbon inert sector.

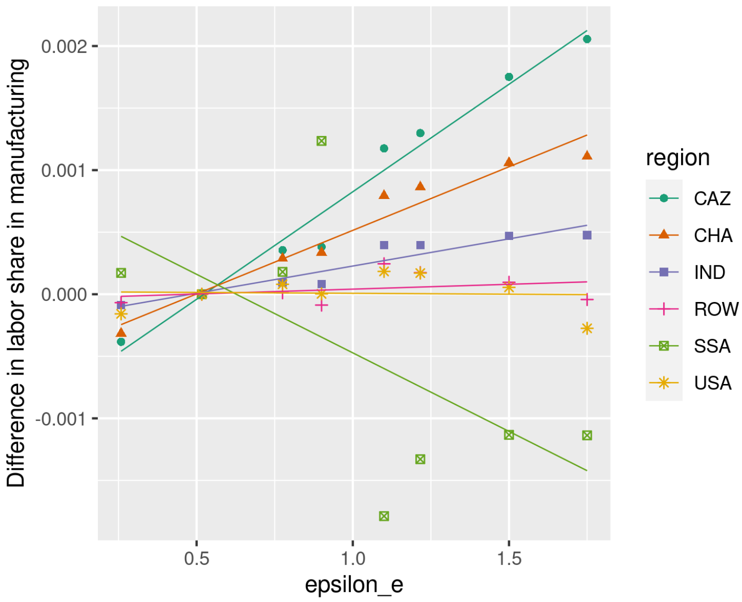

Figure 9: Sensitivity of labor allocation to energy elasticity in the manufacturing sector.

A.6 Mapping from countries to regions

The country to region mapping (illustrated in Fig. 10) contains three regions that are made up of single eponymous country: the United States (USA), Japan (JPN), and India (IND). The other regions are made up as follows:

- **Europe (EUR):** Austria (AUT), Belgium (BEL), Bulgaria (BGR), Croatia (HRV), Cyprus (CYP), Czech Republic (CZE), Denmark (DNK), Estonia (EST), Finland (FIN), France (FRA), Germany (DEU), Greece (GRC), Hungary (HUN), Ireland (IRL), Italy (ITA), Latvia (LVA), Lithuania (LTU), Luxembourg (LUX), Malta (MLT), Netherlands (NLD), Poland (POL), Portugal (PRT), Romania (ROU), Slovakia (SVK), Slovenia (SVN), Spain (ESP), Sweden (SWE), and United Kingdom (GBR)

- **Russia and Reforming Countries (REF):** Armenia (ARM), Azerbaijan (AZE), Belarus (BLR), Georgia (GEO), Kazakhstan (KAZ), Kyrgyzstan (KGZ), Moldova

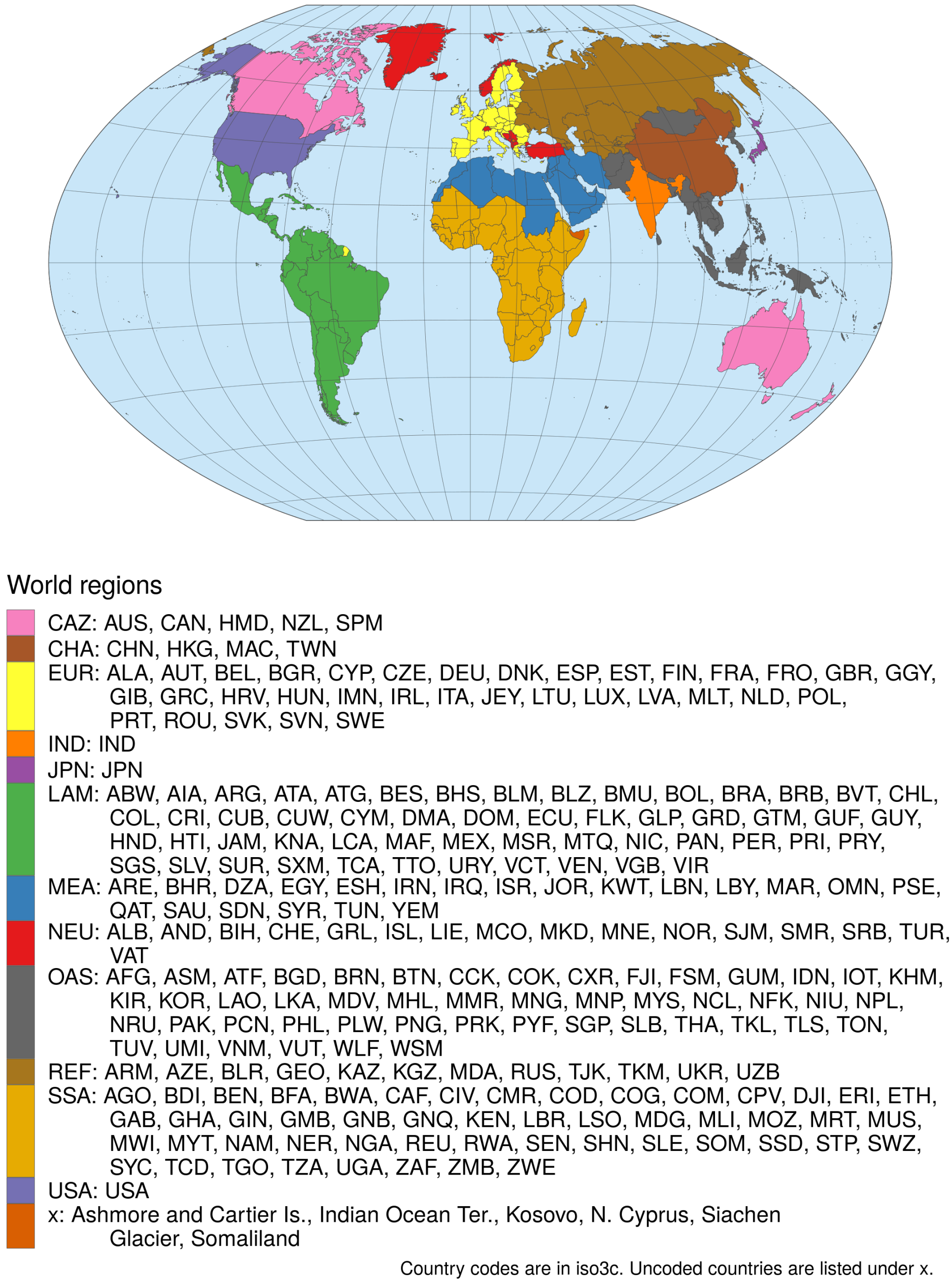

Figure 10: Country to region mapping.

(MDA), Russia (RUS), Tajikistan (TJK), Turkmenistan (TKM), Ukraine (UKR), and Uzbekistan (UZB)

- **Middle Eastern and North Africa (MEA):** Algeria (DZA), Bahrain (BHR), Egypt (EGY), Iran (IRN), Iraq (IRQ), Israel (ISR), Jordan (JOR), Kuwait (KWT), Lebanon (LBN), Morocco (MAR), Oman (OMN), Qatar (QAT), Saudi Arabia (SAU), Sudan (SDN), Syria (SYR), Tunisia (TUN), United Arab Emirates (ARE), and Yemen (YEM)

- **Other Asia (OAS):** Bangladesh (BGD), Butahn (BTN), Brunei (BRN), Cambodia (KHM), Indonesia (IDN), Lao (LAO), Malaysia (MYS), Maldives (MOV), Mongolia (MNG), Myanmar (MMR), Nepal (NPL), Pakistan (PAK), Philippines (PHL), Korea (KOR), Singapore (SGP), Sri Lanka (LKA), Thailand (THA), and Vietnam (VNM)

- **Latin America (LAM):** Anguilla (AIA), Antigua and Barbuda (ATG), Argentina (ARG), Aruba (ABW), Bahamas (BHS), Barbados (BRB), Belize (BLZ), Bolivia (BOL), Brazil (BRA), British Virgin Islands (VGB), Chile (CHL), Colombia (COL), Costa Rica (CRI), Dominica (DMA), Dominican Republic (DOM), Ecuador (ECU), El Salvador (SLV), Grenada (GRD), Guatemala (GTM), Guyana (GUY), Haiti (HTI), Honduras (HND), Jamaica (JAM), Mexico (MEX), Nicaragua (NIC), Panama (PAN), Paraguay (PRY), Peru (PER), Sain Kitts and Nevis (KNA), Saint Lucia (LCA), St Vincent and the Grenadines (VCT), Suriname (SUR), Trinidad and Tobago (TTO), Turks and Caicos Islands (TCA), Uruguay (URY), and Venezuela (VEN)

- **Canada, Australia and New Zealand (CAZ):** Canada (CAN), Australia (AUS), and New Zealand (NZL)

- **Sub-Saharan Africa (SSA):** Angola (AGO), Benin (BEN), Botswana (BWA), Burkina Faso (BFA), Burundi (BDI), Cabo Verde (CPV), Cameroon (CMR), Central African Republic (CAF), Chad (TCD), Comoros (COM), Congo (COD), Côte d'Ivoire (CIV), Democratic Republic of Congo (COD), Djibouti (DJI), Equatorial Guinea (GNQ), Eswatini (SWZ), Ethiopia (ETH), Gabon (GAB), Gambia (GMB), Ghana (GHA), Kenya (KEN), Lesotho (LSO), Liberia (LBR), Madagascar (MDG), Malawi (MWI), Mali (MLI), Mauritania (MRT), Mauritius (MUS), Mozambique (MOZ), Namibia (NAM), Niger (NER), Nigeria (NGA), Rwanda (RWA), Sao Tome and Principe (STP), Senegal (SEN), Seychelles (SYC), Sierra Leone (SLE), South Africa (ZAF), Togo (TGO), Tanzania (TZA), Uganda (UGA), Zambia (ZMB), and Zimbabwe (ZWE)

- **Non-EU European Countries (NEU):** Albania (ALB), Bosnia and Herzegovina (BIH), Iceland (ISL), Montenegro (MNE), Norway (NOR), Serbia (SRB), Switzerland (CHE), Macedonia (MKD), and Turkey (TUR) (Note: the United Kingdom GBR is still classified with EUR)

- **China (CHA):** China (CHN), Hong Kong (HKG), Macao (MAC), and Taiwan (TWN)